IJHAS
International Journal of Health and Allied Sciences
Official Publication of JSS Academy of Higher Education and Research (JSS AHER), Mysuru

Manuscript 1043

Phytochemical and Bioactive Properties of Phlogacanthus and Andrographis Genus Plants: Potential for Post-Pandemic Home Remedies

Patipon Teerakitchotikan

Tibet Tangpao

Supattanakij Posawang

Smitha S. Bhat

Shashanka K. Prasadand

See next page for additional authors

Phytochemical and Bioactive Properties of Phlogacanthus and Andrographis Genus Plants: Potential for Post-Pandemic Home Remedies

Authors

Patipon Teerakitchotikan, Tibet Tangpao, Supattanakij Posawang, Smitha S. Bhat, Shashanka K. Prasadand, and Sarana Rose Sommano

ORIGINAL STUDY

Phytochemical and Bioactive Properties of *Phlogacanthus* and *Andrographis* Genus Plants: Potential for Post-pandemic Home Remedies

Patipon Teerakitchotikan [a,b,1], Tibet Tangpao [b,c,1], Supattanakij Posawang [d], Smitha S. Bhat [b,e], Shashanka K. Prasad [e], Sarana R. Sommano [a,b,*]

[a] Department of Plant and Soil Sciences, Faculty of Agriculture, Chiang Mai University, Chiang Mai 50200, Thailand
[b] Plant Bioactive Compound Laboratory, Faculty of Agriculture, Chiang Mai University, Chiang Mai 50200, Thailand
[c] Office of Research Administration, Chiang Mai University, Chiang Mai 50200, Thailand
[d] Royal Agricultural Research Center, Chiang Mai 313 Moo 12, NongKhwai Sub-district, Hang Dong District, Chiang Mai 50230, Thailand
[e] Department of Biotechnology and Bioinformatics, School of Life Sciences, JSS Academy of Higher Education and Research, Mysore, Karnataka 570015, India

Abstract

This study aimed to differentiate the morphological characteristics, chemical constituents, and bioactive potential of Acanthaceae family plants, specifically three *Phlogacanthus* species and *Andrographis paniculata*. Under identical conditions, cutting stock plant of three *Phlogacanthus* species (Dee pla kung, Hom chang, and Cha hom) and *A. paniculata* (Fah talai jone) were pruned and cultivated at the Chiang Mai Royal Agricultural Research Center. The morphology, biomass yield, and growth rates of the plants were observed after 90 days. Methanolic extracts of the dried aerial parts of these plants were analyzed for bioactive compounds, such as total phenolic content (TPC), total flavonoid content (TFC), total lactone content (TLC), and antioxidant activities (DPPH, ABTS, and FRAP assays). The results revealed that Hom chang had the maximum relative growth rate (RGR) of 2.64×10^{-3} cm/cm/day among the plants, as determined by the morphology analysis. Cha hom and Dee pla kung, on the other hand, had substantially greater biomass yields than the other species. Regarding chemical properties, Dee pla kung exhibited high TPC (13.66 ± 0.10 mg GAE/g), TFC (17.25 ± 0.31 mg CE/g), and TLC ($9.57 \pm 0.59\%$). In addition, Dee pla kung, a species of *Phlogacanthus*, exhibited significant antioxidant activity and was comparable to Fah talai jone (genus *Andrographis*) in terms of biomass yield and chemical properties. These findings lay the groundwork for creating future herbal remedies from local plants and their potential use in the medicinal industry.

Keywords: *Phlogacanthus pulcherrimus*, *P. curviflorus*, *P. thyrsiformis*, *Andrographis paniculate*

1. Introduction

The Acanthaceae family, also known as the Acanthus family, comprises around 229 genera and 3450 species [1,2]. Plants in this family share several common taxonomical characteristics. They are mostly herbs, shrubs, or small trees with simple leaves typically arranged in opposite pairs. Numerous members of this family are used for a great many medicinal purposes [3]. The flowers are typically bisexual and showy, with a two-lipped corolla and two or four stamens that are usually fused to the corolla tube. The fruit is a capsule that may contain numerous small seeds. Members of the Acanthaceae family are widely distributed in tropical and subtropical regions, and many species are valued for their ornamental, medicinal, and economic uses [4–6]. One well-known species,

Received 15 June 2023; revised 21 June 2023; accepted 21 June 2023.
Available online 28 September 2023

* Corresponding author.
E-mail address: sarana.s@cmu.ac.th (S.R. Sommano).
[1] These authors contributed equally as the first author.

https://doi.org/10.55691/2278-344X.1043

Andrographis aniculate, is recognized for its medicinal properties [7–9]. In Thailand, this plant has been recommended for use in primary health care for cases of sore throat and diarrhea, and it has been chosen as an herbal medication for the treatment of common cold symptoms and non-infectious diarrhea [10,11]. In addition, it has been used to remedy complications associated with HIV, hepatitis, diabetes, cancer, kidney disorders, and the Coronavirus Disease 2019 or COVID-19 [12–14]. Similarly, the genus *Phlogacanthus* is found primarily in tropical regions of Asia, and some species, such as *Phlogacanthus pulcherrimus*, *Phlogacanthus cornutus*, *Phlogacanthus thyrsiflorus*, *P. thyrsiformis*, and *Phlogacanthus curviflorus* have traditional medicinal uses in the treatment of various ailments, including fever, inflammation, and skin diseases. They are also clinically reported as having antioxidant, cytotoxic, antimicrobial, analgesic, and anti-inflammatory properties [3,15–19]. *P. pulcherrimus*, *P. curviflorus*, and *P. thyrsiformis* are traditionally cultivated in Thailand for their medicinal properties. The leaves and roots of these plants contain secondary metabolites such as alkaloids, flavonoids, and phenolic compounds, which are believed to be responsible for their therapeutic effects.

The COVID-19 pandemic has led to a surge in demand for natural products and traditional medicine that could be used as treatment and preventive measures. As a result, there has been an increased interest in exploring the pharmacological properties of plants from the Acanthaceae family, including *Phlogacanthus* species, which may offer potential benefits in the fight against COVID-19. Nonetheless, there is no in-depth report regarding the phytochemical compositions of the medicinal plants of the *Phlogacanthus* genus together, with their biological properties, compared with the closer medicinal genus, *Andrographis* [20–22]. Therefore, this research aimed to evaluate the morphological characteristics, chemical compositions, and bioactive potential of the three commonly utilized *Phlogacanthus* genus plants in Thailand, viz., *P. pulcherrimus, P. curviflorus,* and *P. thyrsiformis,* and to evaluate their relationship with their closest sister, *Andrographis paniculate*. The direct outcome of this work is the provision of alternative raw materials for the commercial recovery of natural products that can serve as home remedies in the post-pandemic era. Additionally, these plants may have ecological significance by contributing to preserving biodiversity and ecosystem services.

2. Materials and methods

2.1. Plant materials

Four members of the Acanthaceae family, namely Dee pla kung (DK), Hom chang (HC), Cha hom (CH), and Fah talai jone (FTJ), were cultivated (3 replications) in the plastic nursery bag (6.0×12.0 in) and pot (6.0×4.5 in) from the plant cutting and maintained at the nursery with 70% shade [watering twice a day for 30 min, fertilizing (urea (46-0-0)], in Chiang Mai, Thailand (18.746531, 98.920382). At the initial flowering stage, 50% of the plant canopy was pruned. Then, they were continuously maintained in the nursery for 2 months. Following this, growth performance, viz., plant height, canopy width, and leaf area, was recorded weekly until 4 weeks. The average leaf area was calculated using the following equation according to the ellipsoid shape of the leaf following by Neuweiler, Bertschinger [23];

$$\text{Leaf area } (\text{cm}^2) = 3 \times \Pi \times (\text{length}/2) \times (\text{width}/2)$$

All parameters were analyzed for multiple variables simultaneously to identify the key variables that significantly influence growth performance. Data was computed using principal component analysis (PCA), and the identified influential parameters were used to develop predictive models that can forecast growth performance. Relative growth rate (RGR) was calculated by dividing the difference in ln-transformed plant weight at two harvests by the time difference between those harvests. RGR was estimated by Hoffmann and Poorter [24];

$$\text{Relative growth rate (RGR) (cm/cm/day)} = \ln (W2 - W1)/ (t2 - t1)$$

W1 = initial weight or size W2 = final weight or size t1 = initial time t2 = final time ln = natural logarithm.

At harvest (in March 2022), the aerial parts were collected 3.0 cm above the ground. The yield of fresh weight and dried biomass (g/plant) of leaves and aerial parts were calculated. The taxonomic identities of these plants were described and later sent to the botanist at DOA. The voucher specimen numbers of the plants were preserved at the Plant Bioactive Compound Laboratory, Faculty of Agriculture, Chiang Mai University (CMU).

2.2. Sample preparation and extraction

Prior to extraction, the fresh aerial parts were dried at 60 °C for 2 days using a hot air oven (WGLL-125BE, China) and then ground to a fine powder using a spice grinder at high speed (Spring Green Evolution, PG2500, Thailand). Then, 0.1 g of the air-dried and powdered plant materials were extracted with 1000 μL of 80% (w/w) methanol in a 2.0 mL Eppendorf tube and mixed by a digital ultrasonic cleaner (Jeken PS-10A 2L Ultrasonic Cleaner, USA) for 5 min at room temperature. It was then centrifuged at 5000 × for 15 min. The supernatant was collected, and the procedure was repeated thrice. The supernatant was then adjusted to 5.0 mL with 80% (w/w) methanol in a volumetric flask. The combined supernatant of 500 μL was collected in an Eppendorf tube and evaporated by using a vacuum concentrator (ISS-ENPROTECH UNIVAPO 72-PLACE ROTOR, Thermo Savant, UK) to obtain the crude dried extract [25,26].

2.3. Chemical analysis

2.3.1. Total phenolic content (TPC)

The total phenolic content of the methanolic leaf extract was determined by a spectrophotometric technique using Folin-Ciocalteu method described previously [27,28]. Briefly, 30 μL of the plant extract was added to a 96-well plate, to which 150 μL of 10% Folin-Ciocalteu reagent was added, mixed, and incubated for 7 min 120 μL of a 6% of sodium hydrogen carbonate ($NaHCO_3$) solution was added to the mixture. The 96-well plate was incubated at room temperature in the dark for 60 min, following which the absorbance of the samples was measured at 765 nm using a UV-Vis spectrophotometer (SPECTROstar Nano, BMG LABTECH, Ortenberg, Germany). The assay was performed with a standard solution of gallic acid (0–0.2 mg/mL) to obtain the calibration line. TPC was expressed as milligrams of gallic acid equivalents per gram of extract (mg GAE/g of sample). The samples were prepared in triplicate for each analysis, and the mean absorbance value was obtained.

2.3.2. Total flavonoid content (TFC)

The Total Flavonoid Content was determined by aluminum chloride colorimetric assay [29]. Briefly, 25 μL of plant extracts were added to a 96-well plate and mixed with 125 μL of distilled water. Then, 7.5 μL of 5% $NaNO_2$ solution was added to each well and incubated for 5 min. Following incubation, 15 μL of 10% $AlCl_3$ solution was added, mixed, and incubated for 6 min. Then, 50 μL of 1M NaOH was added to each well. Subsequently, the absorbance at 510 nm was measured using a UV-Vis spectrophotometer. The same procedure was repeated for the catechin standard (from 0 to 0.3 mg/mL), and the calibration curve was constructed. The content of flavonoids in the dried sample was calculated from the equation derived from the standard curve and expressed as catechin equivalent (mg CE/g of the sample).

2.3.3. Total lactone content (TLC)

The total lactone content was evaluated according to the methodology by Aromdee et al. (2005) [5] and Onsa et al. (2022) [30]. Aliquots of the standard *Andrographis paniculata* supplement, which contained 20.0 mg of lactone (20.0 mg, Yanhee Fah Thalai Jone, Bangkok, Thailand) ranging from 0.1 to 1.0 mL were transferred to a test tube and made up to 2.0 mL with ethanol. Afterward, 0.5 mL of 3,5-dinitro benzoic acid and potassium hydroxide reagents were thoroughly missed into each aliquot. 200 μL of the standard solution was transferred into the cuvette, and 50 μL of both dinitrobenzoic acid and potassium hydroxide solution were added. The absorbance of the solution was determined at 536 nm by a UV-Vis spectrophotometer. Plant extracts were analyzed using the same procedure, and the andrographolide content of plant samples was calculated using the standard curve regression equation.

2.3.4. Antioxidant activity

2.3.4.1. 1,1-diphenyl-2-picrylhydrazyl free (DPPH) radical-scavenging activity. DPPH scavenging activity (%) was determined following the method of Norkum ai, Wongkaew [31]. Briefly, the 25 μL of different concentrations of the methanolic extract and 250 μL of 0.1 mM methanolic DPPH solution were added to a 96-well plate. After incubation in the dark at room temperature for 30 min, the absorbance was measured at 517 nm using the UV-Vis spectrophotometer. Methanol (80%) was used as blank. The experiment was repeated three times, and the DPPH scavenging activity was calculated using the following equation;

$$\text{DPPH radical-scavenging activity (\%)} = [A0 - (A1/A0)] \times 100$$

where A0 is the absorbance of the blank, and A1 is the sample absorbance.

2.3.4.2. 2,2′-azino-bis (3-ethylbenzothiazoline-6-sulfonic acid) (ABTS) radical-scavenging activity. The 2,2′-azino-bis(3-ethylbenzothiazoline-6-sulfonic acid)

(ABTS) radical-scavenging activity of the extracts was conducted according to the method of Norkum ai, Wongkaew [31]. The ABTS radical cation was prepared by mixing 7.0 mM ABTS solution with 2.45 mM ammonium persulfate in an equal amount. The mixture was incubated in the dark at room temperature overnight until the solution turned from blue to green. The ABTS radical solution was adjusted with methanol to adsorb 0.700 ± 0.020 at 734 nm. After that, an aliquot of 10 μL of the methanolic extract was mixed with 200 μL of the ABTS working solution and incubated at room temperature for 30 min. After the reaction, the reduction in absorbance at 734 nm was determined using the UV-Vis spectrophotometer. The ABTS value was calculated as follows;

$$\text{ABTS radical-scavenging activity (\%)} = [1 - (A1/A0)] \times 100$$

where A0 is the absorbance of the blank, and A1 is the absorbance of the sample.

2.3.4.3. Ferric reducing/antioxidants power assay (FRAP). The FRAP assay is another method for detecting antioxidant capacity. FRAP reagent was prepared using a previously described method [32,33]. In brief, 300.0 mM acetate buffer (pH 3.6), 10.0 mM TPTZ (2,4,6-tripyridyl-s-triazine) solution in 40.0 mM hydrochloric acid, and 20.0 mM iron (III) chloride were mixed in a 10:1:1 ratio. FRAP reagent (150 μL) was mixed with 20 μL of the sample, 20 μL of 2.0 μM ascorbic acid (positive control), and 20 μL of deionized water (blank) in a 96-well plate. The absorbance of each was measured at 593 nm using a UV-Vis spectrophotometer. The FRAP value was calculated using the following equation:

$$\text{FRAP value} = [(A1 - A0)/(Ac - A0)] \times 2$$

Where Ac is the absorbance of the positive control, A1 is the absorbance of the sample, and A0 is the absorbance of the blank.

2.3.5. Metabolite profiling

LC−MS/MS was performed using an Agilent LC-QTOF 6500 system with an Agilent ZORBAX Eclipse XDB column − C18 (2.1 mm × 50.0 mm, 1.8 μm) [34]. The mobile phase consisted of water (0.1% formic acid), and acetonitrile (with 0.1% formic acid), was used as eluents in a gradient mode. The injection volume was 20 μL of the extract sample extract (1:10 dilution), and the column temperature was maintained at 30 °C. The flow rate was kept constant throughout the gradient. The ultra-performance liquid chromatography (UPLC) system was coupled to a QTOF mass spectrometer (6500 series; Model-G6545B) equipped with an AP-ESI Dual Spray source. Parameters for analysis were set using positive ion mode with spectra acquired over a mass range from *m/z* 120 to 1000. The mass profiling of each plant extract was used as the multivariate data for principal component analysis calculation.

2.4. Statistical Analysis

One-way analysis of variance (ANOVA) and Duncan's multiple range tests at a significance level of 0.05 were conducted to determine the significance of the difference between samples of each plant (SPSS Institute, Armonk, NY, USA). Principal component analysis (PCA) was utilized to summarize the visual differences between the chemical components and biological activities of the extracts, using XLSTAT version 2021.4.1 (Suite NY, New York, NY, USA).

3. Results and discussion

3.1. Taxonomical characteristics and growth parameters

Plant morphology is significant in identifying and understanding taxonomical classification and potential utilization. In this study, four Acanthaceae plants, namely *P. pulcherrimus* (DK), *P. curviflorus* (HC), *P. thyrsiformis* (CH), and *A. paniculate* (FTJ), were investigated for their morphological features (Table 1). DK illustrated with its elongated, elliptic leaves measuring 10.0−15.0 cm long and 4.0−5.0 cm wide. The leaf structure featured pinnately netted venation, an opposite decussate arrangement, and smooth margins. The leaf structure of HC was large, simple, and broad, measuring 15.0−20.0 cm long and 5.0−10.0 cm wide, with an elliptic-broadly obovate shape. The leaf shape was similar to DK, and the margins were entire. CH exhibited elongated leaves measuring 10.0−15.0 cm long and 3.0−4.0 cm wide. These leaves were elliptic in shape and featured a pinnately netted venation, an opposite decussate arrangement, and entire margins. FTJ displayed distinctive characteristics. It had relatively small, lanceolate or ovate-lanceolate leaves measuring 4.0−7.0 cm long and 1.0−3.0 cm wide. These leaves displayed pinnately netted venation, an opposite arrangement, and entire margins. For taxonomical classification within this family, the morphology of the inflorescences plays a crucial role. In the case of DK, the terminal spike inflorescences exhibit bell-shaped or campanulate

Table 1. Morphology of three Phlogacanthus spp. plants and an Andrographis paniculata

Characteristics	DK	HC	CH	FTJ
	Plant morphology			
General				
Leaf structure	Simple leaf long 10.0–15.0 cm and wide 4.0–5.0 cm, elliptic with pinnately netted venation, opposite decussate, and entire margin	Large simple leaf long 15.0 –20.0 cm and wide 5.0–10.0 cm, elliptic-broadly obovate with pinnately netted venation, opposite decussate, and entire margin	Simple leaf long 10.0–15.0 cm and wide 3.0–4.0 cm, elliptic with pinnately netted venation, opposite decussate and entire margin	Simple leaf long 4.0–7.0 cm and wide 1.0–3.0 cm, lanceolate or ovate-lanceolate with pinnately netted venation, opposite and entire margin
Genus	*Phlogacanthus*	*Phlogacanthus*	*Phlogacanthus*	*Andrographis*

DK = Dee pla kung, HC = Hom chang, CH = Cha hom and FTJ = Fah talai jone.

forms with deep red corollas, imparting a distinctive appearance [27]. On the other hand, HC features panicle inflorescences characterized by tubular shapes and brick red corollas, creating a visually captivating display [35]. CH produces thyrsoid panicle inflorescences with tubular shapes and brick red or orange corollas, adding an elegant touch to garden settings [36]. As for FTJ, the terminal raceme inflorescences consist of elongated clusters of flowers, exhibiting a near labiate to bilabiate shape [37]. The flowers are pedicellate, with the fusion of petals forming a tubular or slightly bilabiate corolla.

To compare the growth performance of the *Phlogacanthus* genus (DK, HC, and CH) with the *Andrographis* (FTJ), plant height, canopy width, and leaf area were measured over time, as shown in Table 2. There was a significant expansion in leaf area, indicating robust leaf development. The most substantial leaf expansion was observed approximately three weeks after the initial pruning. Significant differences in plant height and canopy width were observed only in the HC species. This suggests that HC may have unique growth characteristics compared to the other species studied. Furthermore, the complex interactions between the variables affecting growth performance were comprehended by considering multiple parameters simultaneously. Overall, the PCA score plots, which accounted for 65–94% of the data, advised that all recorded parameters influenced the growth performance of both genera (Table 2). It indicated that the plant height, canopy width, and leaf area were recognized as influencing parameters in the same way and could be used to analyze the Relative Growth Rates (RGRs). Therefore, the factors were used to generate predictive models that forecast growth performance, and the relative growth rate was simulated accordingly (Table 3). The results revealed significant differences in the growth rates among the three *Phlogacanthus* spp. plants and the *Andrographis* spp. plant. HC exhibited the highest RGR (2.64×10^{-3} cm/cm/day), followed by CH, while DK had the lowest RGR among the *Phlogacanthus* species. Interestingly, the *Andrographis* spp. plant exhibited the least growth rate (0.37×10^{-3} cm/cm/day). Several factors may contribute to the observed variations in the relative growth rates. Environmental factors such as light availability, temperature, and nutrient availability can significantly influence plant growth rates [38]. Different species may have specific requirements, and optimal growth conditions are variable [39]. Therefore, variations in these factors could explain the differences in growth rates among plants in the *Phlogacanthus* and the *Andrographis* genre.

Table 2. Morphological parameters and principal component analysis (PCA) in loading plots of Phlogacanthus spp. and Andrographis spp. after pruning.

Plant	Plant height	Canopy width	Leaf area	PCA growth parameter
DK	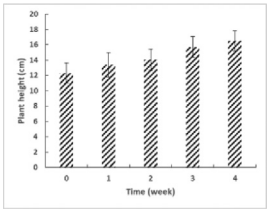	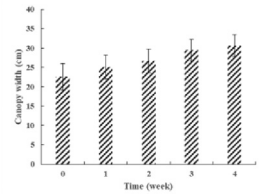	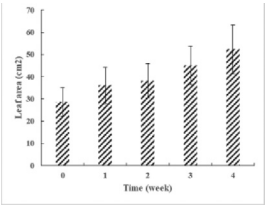	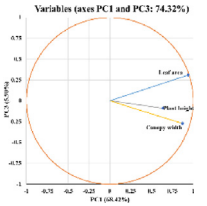
HC	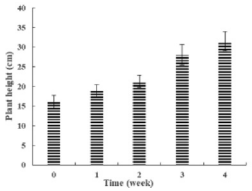	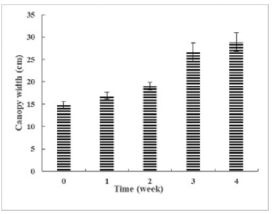	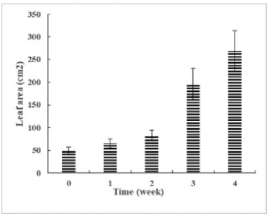	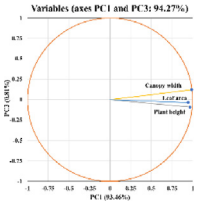
CH	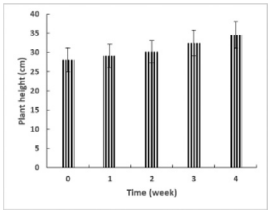	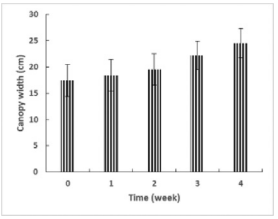	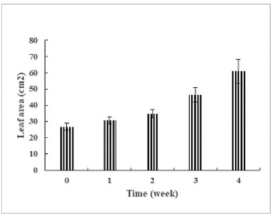	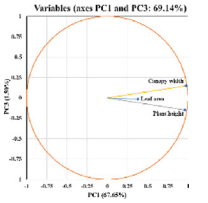
FTJ	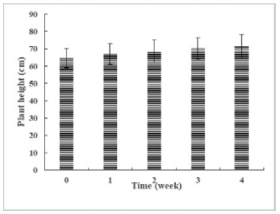	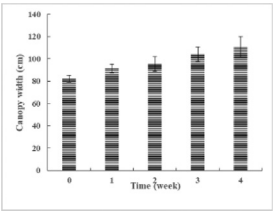	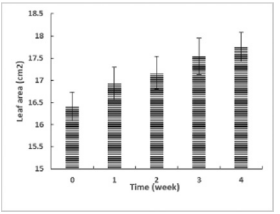	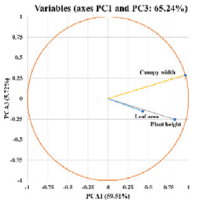

DK = Dee pla kung, HC = Hom chang, CH = Cha hom and FTJ = Fah talai jone.

Table 3. Fresh weight yield, dried biomass weight, and relative growth rates (RGRs) of Phlogacanthus spp. and Andrographis spp.

Plant	Leaf Fresh Weight Yield (g/plant)	Aerial Fresh Weight Yield (g/plant)	Dried Leaf Biomass (g/plant)	Dried Arial Biomass (g/plant)	RGRs (cm/cm/day)
DK	24.21 ± 1.58^{a}	15.71 ± 0.80^{a}	18.59 ± 0.82^{a}	10.69 ± 0.75^{a}	0.80×10^{-3}
HC	7.52 ± 0.63^{b}	12.28 ± 2.00^{ab}	6.16 ± 0.56^{b}	10.07 ± 1.68^{a}	2.64×10^{-3}
CH	29.02 ± 3.78^{a}	17.13 ± 4.80^{a}	22.40 ± 2.83^{a}	12.81 ± 3.57^{a}	1.18×10^{-3}
FTJ	6.16 ± 0.90^{b}	3.87 ± 0.77^{b}	4.84 ± 0.65^{b}	2.71 ± 0.42^{b}	0.37×10^{-3}

The values are shown as mean ± standard error, and different letters indicate significant differences between plant samples at $p = 0.05$. DK = Dee pla kung, HC = Hom chang, CH = Cha hom and FTJ = Fah talai jone.

Moreover, genetic factors could also play a role in determining the growth rates of these plant species. Genetic variations within a species can lead to differences in growth patterns and rates [40]. It is possible that these plants possess different genetic traits that contribute to their observed growth rates. Therefore, variations in these factors could explain the differences in growth rates among plants within *Phlogacanthus* spp. plants and *Andrographis* spp.

Besides growth patterns, evaluating the biomass yield of the edible portion is crucial. Ensuring both its beneficial medicinal properties and its ability to be cultivated on an industrial scale with satisfactory yields are paramount for cultivating medicinal plants [41,42]. Results in Table 3 revealed that DK and CH consistently displayed the highest fresh weight yield and dried biomass. Notably, CH exhibited the highest leaf fresh weight yield of 29.02 ± 3.78 g/plant, an aerial fresh weight yield of 17.13 ± 4.80 g/plant, as well as dried leaf biomass of 22.40 ± 2.83 g/plant, and dried aerial biomass of 12.81 ± 3.57 g/plant. Following this, DK demonstrated a leaf fresh weight yield of 24.21 ± 1.58 g/plant, an aerial fresh weight yield of 15.71 ± 0.80 g/plant, a dried leaf biomass of 18.59 ± 0.82 g/plant, and a dried aerial biomass of 10.69 ± 0.75 g/plant. However, it is worth noting that when considering the fresh aerial weight and dried aerial biomass, HC exhibited values similar to CH and DK while showing relatively lower weights for the leaf parts. This suggests that HC could be a potential candidate for specific applications prioritizing aerial biomass. In contrast, FTJ displayed the lowest yield and biomass parameters among the plants analyzed (also showed in Table 3). It had values of 6.16 ± 0.90 g/plant, 3.87 ± 0.77 g/plant, 4.84 ± 0.65 g/plant, and 2.71 ± 0.42 g/plant for leaf fresh weight yield, aerial fresh weight yield, dried leaf biomass, and dried aerial biomass, respectively. These findings indicate that CH, DK, and HC possess considerable biomass potential, making them promising candidates for industrial cultivation. The variation in biomass among plants within the same genus and species can be attributed to several factors. The organisms' genetic complexity plays a significant role, as different genetic traits can influence the growth and yield of the plants. Additionally, climatic conditions, including sunlight and temperature, profoundly impact the overall growth and biomass production. When grown under favorable conditions, species originating from ruderal or competitive environments tend to exhibit higher relative growth rates (RGRs), indicating a faster increase in biomass per unit of existing biomass [43,44].

3.2. Phytochemical properties

Table 4 displays the phytochemical compositions of plants of the *Phlogacanthus* spp. and compared to the *Andrographis* spp. From the result, DK exhibited the highest total phenolic content (TPC) at 13.66 ± 0.10 mg GAE/g, followed by HC, FTJ, and CH in descending order. Similarly, DK showed the highest total flavonoid content (TFC) at 17.25 ± 0.31 mg CE/g, followed by HC, FTJ, and CH. FTJ contained the total lactone content (TLC) (8.65 ± 0.13%), which can possess various medicinal properties, including antimicrobial, anti-inflammatory, and anticancer activities (41). DK and HC had comparable total lactone content to FTJ (9.57 ± 0.59% and 8.65 ± 0.13%, respectively). Antioxidant activities were assessed using DPPH, ABTS, and FRAP assays, and DK demonstrated the most potent antioxidant capabilities (84.06 ± 0.31% DPPH, 94.23 ± 0.17% ABTS, and 5.88 ± 0.19 FRAP assay). In contrast, CH displayed the lowest antioxidant activities across all three methods (7.18 ± 0.53% DPPH, 75.24 ± 1.45% ABTS, and 1.65 ± 0.13 FRAP assay) and lower levels of phytochemical properties overall. Consequently, DK exhibited significant bioactive compounds comparable to FTJ, indicating its potential as a medicinal plant.

The principal component analysis (PCA) biplot elucidated the intricate interplay between the chemical compositions and plant specimens (Fig. 1). The PCA space was responsible for an impressive 91.69% of the variance in PC1 and an additional 8.23% in PC2, indicating the substantial explanatory power of the model. Notably, the plant

Table 4. Phytochemical properties of Phlogacanthus spp. and Andrographis spp.

Plant	TPC (mg GAE/g)	TFC (mg CE/g)	TLC (%)	DPPH (%)	ABTS (%)	FRAP
DK	13.66 ± 0.10^{a}	17.25 ± 0.31^{a}	9.57 ± 0.59^{a}	84.06 ± 0.31^{a}	94.23 ± 0.17^{a}	5.88 ± 0.19^{a}
HC	9.47 ± 1.04^{b}	8.56 ± 0.62^{c}	7.24 ± 0.84^{b}	49.29 ± 1.59^{c}	94.31 ± 0.08^{a}	4.68 ± 0.52^{b}
CH	3.70 ± 0.12^{c}	4.03 ± 0.28^{d}	4.42 ± 0.84^{c}	7.18 ± 0.53^{d}	75.24 ± 1.45^{b}	1.65 ± 0.13^{c}
FTJ	8.28 ± 0.52^{b}	10.97 ± 0.49^{b}	8.65 ± 0.13^{ab}	74.11 ± 1.21^{b}	93.63 ± 0.06^{a}	5.63 ± 0.32^{ab}

The values are shown as mean ± standard error, and different letters indicate significant differences between plant samples at $p = 0.05$. DK = Dee pla kung, HC = Hom chang, CH = Cha hom, and FTJ = Fah talai jone; TPC = Total phenolic content, TFC = Total flavonoid content, and TLC = Total lactone content.

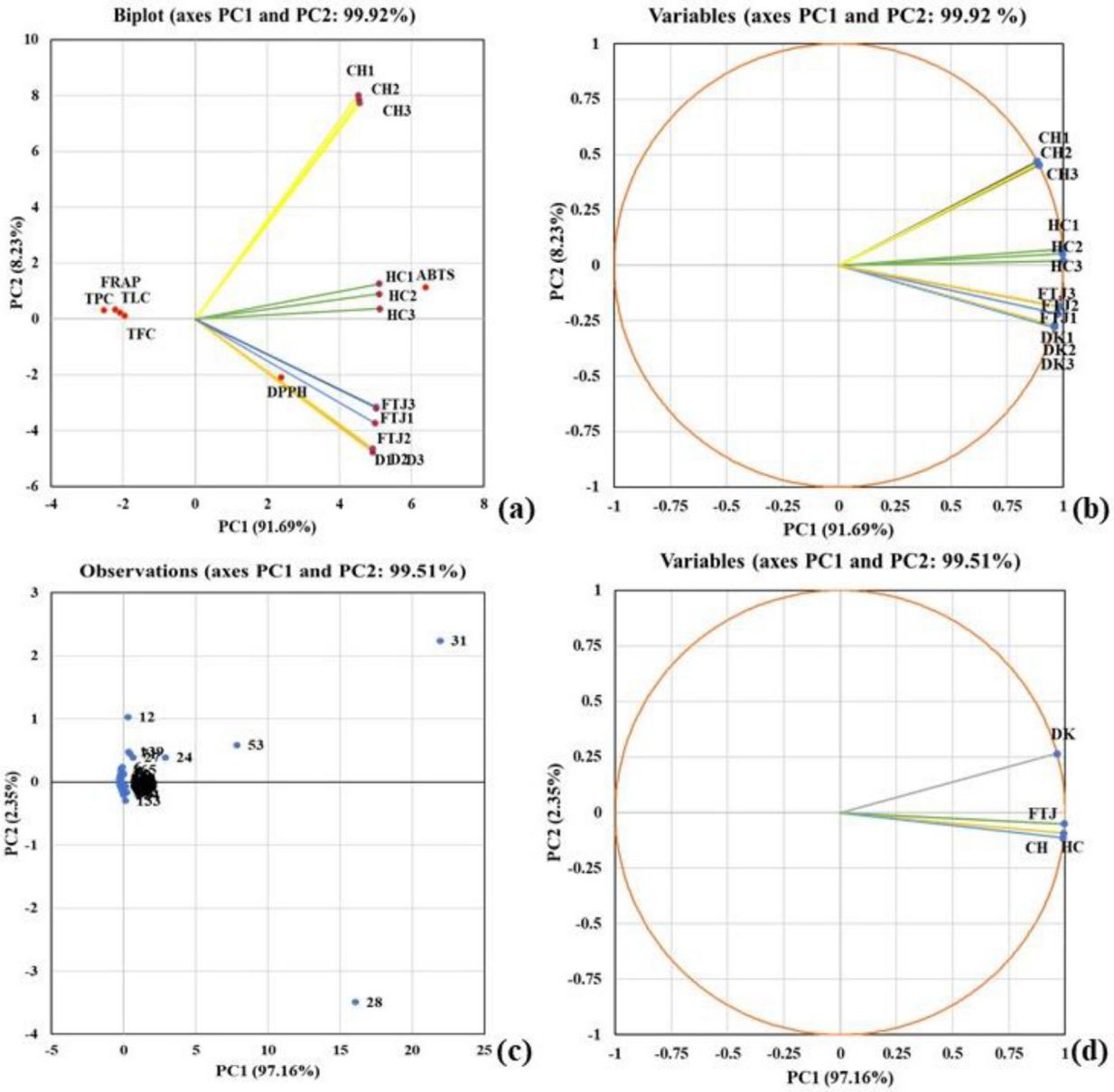

Fig. 1. Principal component analysis (PCA) of Phlogacanthus spp. and Andrographis spp. based on their phytochemical properties and metabolite profiling. DK = Dee pla kung, HC = Hom chang, CH = Cha hom, and FTJ = Fah talai jone; (a) biplot of chemical properties with the samples, (b) loading plot of the samples, (c) score plot of metabolites (the code number refers to metabolites 1-212 in supplementary table 1); and (d) loading plot of the samples.

samples exhibited discernible patterns that allowed for their classification into three distinct relationships based on their chemical compositions. The first relationship encompassed DK and FTJ, demonstrating remarkable proximity to % DPPH, suggesting a strong association between these plants and their chemical compositions. Conversely, the second relationship involved HC, which was closest to %ABTS, indicating its specific affinity for this chemical attribute. In contrast, CH was characterized by the lowest values across all chemical properties compared to the other plants, implying its distinct chemical profile within the dataset. Furthermore, it is worth noting that this plant family consistently displayed normal levels of TPC, TFC, TLC, and FRAP values, underscoring the typical presence of these chemical markers in this particular botanical family. A notable correlation exists between the overall quantity of phenolic and flavonoid compounds and the antioxidant capacity of plants. Phenolic and flavonoid compounds are secondary metabolic products synthesized by plants and contribute to their antioxidant properties [45,46]. There is novel research on *A. paniculata* which showed the chemical properties of lactones, phenolic, flavonoid, and antioxidant activities similar to this study [30]. These values of *Phlogacanthus* species, belonging to the Acanthaceae family, were also reported by other studies. For example, *P. pubinervius* had the amount of phenol content, flavonoid content, and DPPH scavenging activity with 95.35 mg/g, 29.27 mg/g, and 77.83%, respectively. Also, *P. jenkinsii* showed 357.72% of DPPH scavenging activity [15,47]. Compared with the previous studies, According to Poeaim et al. (2016) [27], reported that the total phenolic contents and antioxidant activity (DPPH and ABTS assays) of water crude extract from *P. pulcherrimus* were 13.77 mg GAE/g extract, 9.87%, and 23.06%, respectively, which is closely related to our result. Nevertheless, the study of Kripasana and Xavier (2020) [47] showed that the methanolic crude of *P. thyrsiflorus* and *P. curviflorus* gave a higher phenol content (100.56 mg/g extract and 99.56 mg/g extract, respectively), flavonoid content (31.43 mg/g extract and 35.51 mg/g extract respectively) and DPPH scavenging activity (92.94% and 94.20% respectively). These were probably due to the different areas and conditions of cultivation and the extraction method [48]. Additionally, it is important to acknowledge that although plants may have similar levels of phenolic and flavonoid compounds and antioxidant capacity, these factors may not directly correlate with growth parameters and biomass [43]. The variation in relative growth rate among plant species within this family can be attributed to inherent differences in their chemical composition rather than solely relying on the levels of phenolic and flavonoid compounds or antioxidant capacity. Therefore, when studying plants' growth dynamics and biomass production within this family, it is essential to consider other factors beyond phytochemical content [49].

3.3. Metabolite profiling

The LC-MS analysis revealed 212 distinct metabolites within the volatile and nonvolatile organic compounds, which have been comprehensively documented in Supplementary Table 1. The loading plot generated from the PCA analysis exhibited a substantial variance distribution, with PC1 accounting for 97.16% and PC2 contributing 2.35% of the total variance (Fig. 1). This scoring plot effectively highlighted the variations in metabolite compounds across all plants (Fig. 1c), facilitating the grouping of specimens based on their quantitative data (Fig. 1d). As indicated by their distinct positions on the loading plot, CH, HC, and FTJ exhibited a clear trend of higher levels of similar metabolic compounds. In particular, among these metabolites was oleamide [28], a fatty acid derivative derived from oleic acid, a monounsaturated fatty acid commonly found in plants [50]. Conversely, CH exhibited significant dissimilarity from the other plant samples, suggesting a notable deviation in its metabolic profile (Fig. 1d). DK was dominated by 2-tetradecanone [12], 6,10,14-trimethyl-5,9,13-pentadecatrien-2-one [24], sphinganine [53] and phytosphingosine [31]. Two of these compounds, 2-tetradecanone and 6,10,14-trimethyl-5,9,13-pentadecatrien-2-one, are ketones [51,52]. Sphinganine and phytosphingosine, on the other hand, are both sphingolipids—a class of lipids with essential functions in membrane structure and signaling [53]. The significant dissimilarity from the other plant samples of DK suggested a notable deviation in its metabolic profile. Plant secondary metabolites assume pivotal roles in the survival of plants and in establishing intricate ecological interdependencies with other species [54]. The utilization of plant secondary

metabolites not only serves as critical primary metabolites but also holds significant potential in medicine. These compounds play a vital role in enhancing plant growth, particularly under diverse environmental stresses [55]. Additionally, their application extends beyond plant physiology, as plant secondary metabolites have demonstrated valuable medicinal properties. The exploration and utilization of these metabolites in the medical field open up possibilities for developing novel drugs, therapies, and treatments, harnessing the beneficial effects derived from the intricate biochemical pathways of plants. Therefore, plant secondary metabolites serve as essential components in plant growth optimization and their applied use in the advancement of medical science. Within this context, the plant species belonging to the Acanthaceae family assume a pivotal role treating various illnesses. These plants are renowned for their rich reservoir of essential secondary metabolites such as alkaloids, phenols, terpenoids, tannins, quinones, cardiac glycosides, saponins, carbohydrates, flavonoids, and proteins [56,57]. These compounds possess diverse therapeutic properties, making them valuable resources for developing new medicines. Utilizing these plant secondary metabolites not only enhances plant growth and resilience but also offers immense potential for discovering novel treatments and therapies in the medical field. Exploring of the secondary metabolites in medicinal plants of the Acanthaceae family opens up new avenues for addressing critical health challenges and improving human well-being.

4. Conclusion

In conclusion, this study successfully distinguished the morphological characteristics, chemical compositions, and bioactive potential of various plants from the Acanthaceae family, including three *Phlogacanthus* species and *Andrographis paniculata*. The results revealed that Hom chang exhibited the highest relative growth rate among the plants, while Cha hom and Dee pla kung displayed significantly higher biomass yields. Notably, Dee pla kung, a *Phlogacanthus* species, showcased remarkable levels of phenolic, flavonoid, and lactone content. Additionally, its antioxidant activities were noteworthy, comparable to Fah talai jone from the *Andrographis* genus. These findings offer valuable preliminary insights into these plants' potential utilization and value addition in both the medicinal and agricultural industries.

Contribution details

Conceptualization: S.R.S.; methodology: P.T. and T.T.; validation: T.T.; formal analysis: P.T., T.T., S.S.B. and S.K.P.; investigation: P.T.; resources: S.P., S.R.S. and S.K.P.; data curation: P.T., S.S.B and S.K.P; writing—original draft preparation: P.T. and T.T.; writing—review and editing: S.P., S.K.P., S.S.B. and S.R.S.; visualization: P.T., T.T. and S.R.S.; supervision: S.R.S.; project administration: S.P., S.K.P. and S.S.B; funding acquisition: S.R.S. All authors have read and agreed to the published version of the manuscript.

Acknowledgements

P.T., T.T., S.R.S. would like to thank the Faculty of Agriculture, Chiang Mai University, for the infrastructure provided. P.T. would like to acknowledge the Ph.D. program in Horticulture, Faculty of Agriculture, Chiang Mai University, under the CMU Presidential Scholarship. S.P. would like to acknowledge Royal Agricultural Research Center, Chiang Mai for their support. S.S.B and S.K.P. would like to thank the Department of Biotechnology and Bioinformatics, JSS Academy of Higher Education and Research, Mysuru for the infrastructure and support received.

Conflict of Interest

The authors declare no conflict of interest and all authors are in agreement to publish this article in the International Journal of Health and Allied sciences.

Appendix

Supplementary table 1. The metabolite compounds by using LC-MS of Phlogacanthus spp. and Andrographis spp. plants.

No.	Chemical compounds	Chromatogram peak area			
		DK	HC	CH	FTJ
1	Betaine	nd	3.44×10^4	nd	nd
2	Aminocaproic acid	nd	nd	4.94×10^3	nd
3	Phenylpropiolic acid	1.01×10^4	nd	nd	nd
4	(E)-3-(2-Hydroxyphenyl)-2-propenal	1.11×10^4	2.11×10^4	2.52×10^4	nd
5	DL-2-amino-octanoic acid	1.47×10^4	1.47×10^4	nd	nd
6	3-Hydroxycoumarin	1.73×10^4	nd	nd	7.56×10^3
7	D-(+)-3-Phenyllactic acid	4.87×10^3	1.60×10^4	1.45×10^4	nd
8	Triethyl phosphate	4.44×10^3	5.60×10^3	5.61×10^3	4.56×10^3
9	2,6-Dimethoxy-4-propylphenol	3.77×10^3	3.77×10^3	2.76×10^3	nd
10	3,5,6-Trichloro-2-pyridinol	3.73×10^3	3.45×10^3	3.73×10^3	3.56×10^3
11	dodecanamide	nd	nd	nd	4.21×10^3
12	2-Tetradecanone	6.74×10^4	nd	nd	nd
13	2-(4-Methyl-5-thiazolyl) ethyl butanoate	6.16×10^2	nd	nd	nd
14	Tyrosol 4-sulfate	nd	5.07×10^2	7.05×10^2	nd
15	2-Pentadecanone	nd	nd	nd	4.08×10^3
16	Hexanal octane-1,3-diol acetal	5.26×10^3	7.37×10^3	nd	nd
17	2,6-Di-tert-butyl-4-ethylphenol	2.54×10^3	nd	2.40×10^3	nd
18	CGP 52608	nd	nd	nd	4.59×10^2
19	Acetyl Tyrosine Ethyl Ester	nd	3.91×10^3	nd	nd
20	Herculin	nd	7.15×10^3	nd	nd
21	Palmitic amide	3.79×10^3	nd	nd	nd
22	Falcarindione	nd	nd	nd	5.89×10^3
23	Cicutoxin	nd	nd	nd	5.69×10^3
24	6,10,14-Trimethyl-5,9,13-pentadecatrien-2-one	1.07×10^5	1.04×10^5	1.03×10^5	1.02×10^5
25	Capsi-amide	1.81×10^3	nd	2.20×10^3	nd
26	ar-Artemisene	nd	9.38×10^3	nd	nd
27	16-hydroxy hexadecanoic acid	4.67×10^4	7.06×10^4	nd	nd
28	C16 Sphinganine	2.79×10^5	6.31×10^5	6.70×10^5	5.97×10^5
29	Asp–Phe	nd	1.82×10^4	nd	nd
30	10-Eicosene	nd	3.05×10^3	nd	2.53×10^3
31	Oleamide	7.17×10^5	6.93×10^5	7.34×10^5	7.55×10^5
32	Citronellyl cinnamate	nd	nd	nd	1.76×10^3
33	Neoabietal	4.62×10^3	nd	4.92×10^4	nd
34	1-Octen-3-yl glucoside	nd	2.80×10^3	1.69×10^3	nd
35	Aphidicolan-16beta-ol	1.42×10^3	nd	1.44×10^3	nd
36	(S)-3-Octanol glucoside	nd	9.53×10^2	nd	nd
37	Nordihydrocapsiate	8.40×10^2	nd	nd	nd
38	(R)-Prunasin	2.45×10^3	nd	6.22×10^3	nd
39	5-Methoxy-1,7-diphenyl-3-heptanone	nd	nd	nd	1.42×10^4
40	Spiroxamine	4.63×10^3	nd	nd	nd
41	Juvocimene 2	nd	nd	nd	5.72×10^3
42	Coelogin	nd	nd	nd	2.29×10^3
43	17alpha-Methyl-17beta-hydroxyandrosta-4,6-dien-3-one	nd	nd	nd	3.99×10^3
44	5alpha-Androstane-3,11,17-trione	nd	nd	nd	1.43×10^3
45	17beta-Hydroxy-4alpha-methyl-5alpha-androstan-3-one	nd	nd	3.65×10^3	nd
46	1-(beta-D-Glucopyranosyloxy)-3-octanone	3.75×10^3	3.75×10^3	nd	nd
47	5-O-Methylembelin	nd	nd	nd	2.56×10^3
48	N-Feruloyltyramine	nd	2.54×10^3	nd	nd
49	(+)-Prosopinine	6.46×10^3	7.56×10^3	nd	2.24×10^3
50	Litcubinine	nd	1.26×10^3	nd	nd
51	10-Hydroxyestra-1,4-dien-3-one acetate	2.03×10^3	2.47×10^3	nd	4.45×10^3

(*continued on next page*)

Supplementary table 1. (continued)

No.	Chemical compounds	Chromatogram peak area			
		DK	HC	CH	FTJ
52	17beta-Hydroxy-17-methylandrost-4-ene-3,11-dione	7.59×10^3	nd	nd	2.01×10^3
53	Phytosphingosine	2.54×10^5	2.64×10^5	2.92×10^5	2.52×10^5
54	4,5alpha-Dihydro-2-(hydroxymethylene) testosterone	nd	nd	1.33×100^4	9.03×10^3
55	Chlorpyrifos-methyl	1.26×10^3	1.12×10^3	1.28×10^3	1.24×10^3
56	epi-Tulipinolide diepoxide	nd	7.24×10^2	nd	nd
57	Austroinulin	nd	nd	1.19×10^3	nd
58	N-(14-Methylhexadecanoyl) pyrrolidine	nd	nd	1.29×10^3	7.17×10^2
59	Decylubiquinol	1.47×10^4	nd	1.23×10^4	1.25×10^4
60	Ethylvanillin glucoside	nd	2.68×10^3	4.16×10^3	nd
61	12-Methoxy-8,11,13-abietatrien-20,11-olide	nd	nd	nd	7.44×10^2
62	13-Hydroxy-2-(hydroxymethylene)-3-oxo-13,17-seco-5alpha-androstan-17-oic acid, delta-lactone	nd	2.90×10^4	nd	2.55×10^3
63	17-Oxogrindelic acid	nd	nd	nd	4.07×10^3
64	$6\tilde{I}^2$, $7\tilde{I}^2$ -Dihydroxykaurenoic acid	nd	nd	nd	6.61×10^4
65	3-O-p-Coumaroylquinic acid	4.08×10^3	nd	nd	nd
66	cis-Cetoleic acid	nd	8.61×10^2	8.83×10^2	nd
67	Docosanamide	nd	3.18×10^3	3.61×10^3	3.01×10^3
68	Polyoxyethylene (600) mono- ricinoleate	3.96×10^3	2.97×10^3	3.37×10^3	2.34×10^3
69	6-Hydroxy-8-docosanone	1.31×10^3	nd	nd	nd
70	Inulobiose	3.53×10^3	nd	nd	nd
71	10,20-Dihydroxyeicosanoic acid	4.36×10^4	4.71×10^4	nd	nd
72	2,4,12-Octadecatrienoic acid piperidide	1.11×10^3	6.16×10^2	1.35×10^3	1.45×10^3
73	6beta,11alpha-Dihydroxyprogesterone	nd	7.40×10^2	nd	8.21×10^2
74	Calycanthine	nd	nd	nd	1.55×10^3
75	15-dehydro-prostaglandin I2	nd	nd	nd	6.54×10^3
76	13,14-Dihydro-15-keto-PGE2	nd	nd	nd	1.73×10^3
77	20-hydroxy LTB4	nd	nd	nd	1.41×10^3
78	Cis-5-Caffeoylquinic acid	nd	nd	nd	3.08×10^3
79	Gravacridonediol methyl ether	nd	3.26×10^3	1.11×10^3	nd
80	Catalpol	nd	nd	nd	2.81×10^3
81	Cardiopetalidine	nd	9.11×10^2	nd	nd
82	Tetrahydrocortisone	nd	nd	nd	1.02×10^3
83	19(R)-hydroxy-PGE2	nd	nd	nd	6.28×10^2
84	Blumenol C glucoside	nd	nd	3.49×10^3	nd
85	Pipereicosalidine	nd	nd	nd	7.98×10^2
86	Misoprostol	9.23×10^2	9.63×10^2	9.08×10^2	1.19×10^3
87	Porson	1.38×10^3	1.50×10^3	9.52×10^2	3.16×10^3
88	Surinamensin	nd	nd	nd	2.09×10^3
89	Rehmaionoside C	nd	1.36×10^3	nd	nd
90	Drotaverine	nd	6.30×10^2	nd	nd
91	Pipazethate	nd	nd	3.40×10^2	nd
92	Acetyl tributyl citrate	4.65×10^3	4.65×10^3	nd	nd
93	Aminopentol	3.97×10^3	2.39×10^3	3.37×10^3	3.53×10^3
94	Morroniside	nd	3.83×10^3	2.70×10^3	3.27×10^3
95	(1R,3R,4R,5S,6S,8x)-1-Acetoxy-8-angeloyloxy-3,4-epoxy-5-hydroxy-7(14),10-bisaboladien-2-one	nd	nd	nd	7.83×10^2
96	Lincomycin	nd	nd	1.02×10^3	nd
97	Erysothiopine	8.72×1002	3.60×10^3	1.65×10^3	4.72×10^3
98	Armillaripin	4.05×10^3	2.14×10^3	nd	5.55×10^3
99	Istamycin B1	nd	6.97×10^2	nd	nd
100	11beta,17,21-Trihydroxy-2alpha-methylpregn-4-ene-3,20-dione 21-acetate	nd	nd	1.55×10^3	nd
101	Dimethyl 3-methoxy-4-oxo-5-(8,11,14-pentadeca-trienyl)-2-hexenedioate	nd	nd	2.66×10^2	nd
102	1-Octen-3-yl primeveroside	nd	5.48×10^3	nd	nd
103	Austalide L	2.15×10^3	3.01×10^3	3.13×10^3	3.31×10^3
104	Solanocapsine	1.67×10^3	nd	nd	1.55×10^3
105	Kaempferol 3-O-alpha-L-rhamnofuranoside	1.28×10^3	nd	nd	nd
106	Propylene glycol alginate	nd	7.99×10^2	nd	nd

(*continued on next page*)

Supplementary table 1. (continued)

No.	Chemical compounds	Chromatogram peak area			
		DK	HC	CH	FTJ
107	Glucorhein	nd	6.11×10^2	nd	nd
108	Stigmastentriol	2.45×10^3	1.80×10^3	2.84×10^3	nd
109	(ent-2b,4S,9a)-2,4,9-Trihydroxy-10(14)-oplopen-3-one 2-(2-methylbutanoate) 9-(3-methyl-2E-pentenoate)	2.91×10^3	nd	4.70×10^2	nd
110	4-Hydroxyvalsartan	8.53×1002	nd	nd	nd
111	10-Deoxymethymycin	7.49×10^2	2.74×10^2	6.29×10^2	7.63×10^2
112	Lucidenolactone	6.28×10^2	1.13×10^3	1.06×10^3	1.37×10^3
113	Militarinone A	2.40×10^3	3.86×10^3	3.80×10^3	nd
114	Wistin	nd	nd	nd	1.05×10^3
115	3-Methylellagic acid 8-rhamnoside	2.59×10^3	nd	nd	1.35×10^3
116	10-Desacetyltaxuyunnanin C	1.71×10^3	nd	nd	nd
117	Withanolide A	nd	5.01×10^3	4.88×10^3	nd
118	Ximelagatran	2.67×10^3	nd	5.67×10^2	nd
119	11-Deacetylvaltrate 11-(3-hydroxy-3-methylbutanoate)	nd	1.04×10^3	nd	nd
120	Fusicoccin H	8.43×10^2	nd	nd	nd
121	Cer(d18:0/12:0)	1.62×10^3	1.60×10^3	2.39×10^3	nd
122	Stigmatellin Y	1.54×10^3	1.51×10^3	nd	1.42×10^3
123	Goshonoside F1	1.67×10^3	nd	1.87×10^3	1.84×10^3
124	4′,5,6-Trimethylscutellarein 7-glucoside	nd	2.76×10^4	1.36×10^4	nd
125	Hemibrevetoxin B	nd	nd	2.50×10^4	nd
126	Glutathionylspermine	nd	nd	2.26×10^3	nd
127	Harpagoside	4.45×10^2	5.52×10^2	nd	nd
128	7,11-Bisdeacetylvaltrate 7-(3-methylpentanoate) 11-(3-hydroxy-3-methylbutanoate)	nd	8.12×10^2	nd	nd
129	Cucurbitacin S	nd	1.26×10^3	nd	1.10×10^3
130	Mupirocin	2.05×10^3	nd	nd	nd
131	Cavipetin B	nd	nd	nd	3.06×10^4
132	6F-alpha-D-Galactosylsucrose	2.35×10^3	nd	nd	nd
133	(5alpha,6beta,14alpha,20R,22R)-5,6,14,20,27-Pentahydroxy-1-oxowith-24-enolide	9.77×10^2	nd	5.81×1004	nd
134	Veracevine	8.63×10^2	nd	nd	nd
135	Carindone	nd	2.19×10^3	nd	nd
136	11a,12a-Epoxy-3b-hydroxy-28,13-oleananolide 3-acetate	4.61×10^2	5.24×10^2	4.68×10^2	5.76×10^2
137	dTDP-4-amino-2,3,4,6-tetradeoxy-D-glucose	nd	1.99×10^3	nd	nd
138	S-(Hydroxymethyl)mycothiol	nd	2.98×10^3	8.35×10^3	nd
139	Luteone 7-glucoside	4.21×10^4	3.49×10^4	nd	nd
140	L-Olivosyl-oleandolide	nd	nd	1.83×10^3	nd
141	Citrusin F	nd	5.89×10^2	nd	nd
142	Withaperuvin D	3.33×10^3	nd	nd	nd
143	24,25-Diacetylvulgaroside	4.88×10^2	nd	nd	nd
144	Tridodecylamine	1.17×10^3	1.06×10^3	nd	nd
145	Physangulide	nd	nd	2.56×10^4	1.14×10^3
146	Tetrahydro-6-(2-hydroxy-16,19-dimethylhexacosyl)-4-methyl-2H-pyran-2-one	nd	nd	8.62×10^2	nd
147	(24E)-3alpha-Acetoxy-15alpha-hydroxy-23-oxo-7,9(11),24-lanostatrien-26-oic acid	4.71×10^2	4.26×10^2	nd	nd
148	L-Oleandrosyl-oleandolide	nd	7.99×10^2	nd	nd
149	Sabadelin	4.66×10^3	1.30×10^4	8.00×10^3	nd
150	Corchoroside A	1.85×10^3	nd	nd	nd
151	Ganoderic acid L	1.73×10^3	nd	nd	nd
152	N-Palmitoylsphingosine	3.41×10^2	nd	3.86×10^2	nd
153	(5b,7a,12a)-2-(3-methoxyphenyl)-2-oxoethyl ester-7,12-dihydroxy-cholan-24-oic acid	nd	nd	1.62×10^3	nd
154	Hovenidulcigenin A	2.75×10^2	3.07×10^2	nd	3.23×10^2
155	Puerarin xyloside	nd	nd	nd	6.34×10^2
156	Cymarin	nd	nd	1.38×10^4	nd
157	Bipindogulomethyloside	2.78×10^3	nd	nd	nd
158	Armillaramide	nd	3.33×10^3	nd	nd

(*continued on next page*)

Supplementary table 1. (continued)

No.	Chemical compounds	Chromatogram peak area			
		DK	HC	CH	FTJ
159	Cucurbitacin E	5.53×10^2	nd	nd	nd
160	Epomusenin A	nd	1.95×10^3	nd	2.15×10^3
161	Canescein	nd	1.07×10^3	nd	3.02×10^3
162	y-Morphine	nd	nd	5.18×10^2	nd
163	Ganodermic acid P2	nd	1.79×10^2	nd	1.93×10^2
164	1,1'-(1,4-Dihydro-4-nonyl-3,5-pyridinediyl) bis[1-dodecanone]	5.72×10^2	6.41×10^2	5.82×10^2	6.38×10^2
165	Asclepin	1.35×10^4	nd	nd	nd
166	Isofucosterol glucoside	1.06×10^3	nd	nd	nd
167	Epicatechin-(2beta->7,4beta->6)-catechin	6.91×10^2	8.82×10^2	7.14×10^2	1.05×10^3
168	beta-Sitosterol 3-O-beta-D-galactopyranoside	2.08×10^3	1.50×10^3	1.74×10^3	nd
169	(+)-7-epi-Syringaresinol 4′-glucoside	nd	6.35×10^2	7.27×10^2	nd
170	DG (15:0/18:0/0:0)	nd	nd	4.74×10^2	nd
171	Antibiotic X 14889A	nd	nd	nd	3.54×10^2
172	Sandoricin	nd	nd	nd	1.97×10^4
173	Avermectin B2b aglycone	nd	nd	2.42×10^2	nd
174	Pheophorbide a	4.78×10^3	1.77×10^3	nd	nd
175	Peonidin 3-lathyroside	6.88×10^2	nd	nd	nd
176	Landomycin D	nd	9.80×10^2	nd	nd
177	Kaempferol 3-rhamnoside 7-galacturonide	nd	nd	4.57×10^3	nd
178	Harderoporphyrin	1.01×10^3	nd	nd	nd
179	BQ 123	nd	nd	7.57×10^2	nd
180	DG (22:5(4Z,7Z,10Z,13Z,16Z)/14:1(9Z)/0:0)	nd	nd	nd	1.10×10^3
181	Genistein 4′,7-O-diglucuronide	nd	2.06×10^3	nd	nd
182	R.g.-Keto III	6.31×10^2	nd	nd	nd
183	Goshonoside F4	9.46×10^2	nd	1.83×10^3	nd
184	(3a,5b,7a,12a)-24-[(carboxymethyl)amino]-1,12-dihydroxy-24-oxocholan-3-yl-b-D-Glucopyranosiduronic a	1.40×10^3	nd	nd	nd
185	Capsianoside IV	nd	nd	2.61×10^2	nd
186	Lyciumoside VIII	nd	nd	6.23×10^2	nd
187	Aridanin	nd	7.98×10^2	6.28×10^2	7.44×10^2
188	3-O-trans-Feruloyleuscaphic acid	nd	nd	nd	2.79×10^2
189	(S)-Nerolidol 3-O-[a-L-Rhamnopyranosyl-(1->4)-a-L-rhamnopyranosyl-(1->2)-b-D-glucopyranoside]	8.82×10^2	5.25×10^2	1.18×10^3	3.66×10^2
190	Lasonolide A	nd	nd	nd	1.43×10^3
191	Boivinide A	nd	nd	7.67×10^2	nd
192	Cheirotoxol	4.01×10^2	nd	nd	nd
193	1,2 di-(9Z,12Z,15Z-octadecatrienoyl)-3-O-Beta-D-galactosyl-sn-glycerol	nd	9.85×10^2	nd	3.84×10^2
194	Oligomycin A	nd	1.14×10^3	6.41×10^2	7.42×10^2
195	Telithromycin	nd	4.46×10^2	5.87×10^2	nd
196	Quillaic acid 3-[galactosyl-(1->2)-glucuronide]	nd	1.70×10^2	nd	nd
197	Leucomycin A3	nd	2.15×10^2	4.61×10^2	nd
198	(3b,21b)-12-Oleanene-3,21,28-triol 28-[arabinosyl-(1->3)-arabinosyl-(1->3)-arabinoside]	nd	nd	2.50×10^2	nd
199	Pectenotoxin 2	1.68×10^2	nd	nd	nd
200	Hebevinoside VIII	nd	nd	nd	1.73×10^2
201	TG(18:1(9Z)/16:0/20:5(5Z,8Z,11Z,14Z,17Z))[iso6]	1.54×10^2	nd	nd	nd
202	3″-Adenylylstreptomycin	3.87×10^2	nd	nd	nd
203	28-[Glucosyl-(1->6)-glucosyl]oleanolic acid 3-arabinoside	nd	8.91×10^2	nd	nd
204	Glycerol 2-(9Z,12Z-octadecadienoate) 1-hexadecanoate 3-O-[alpha-D-galactopyranosyl-(1->6)-beta-D-galactopyranoside]	nd	nd	nd	7.69×10^2
205	TG(18:2(9Z,12Z)/18:0/22:6(4Z,7Z,10Z,13Z,16Z,19Z))[iso6]	3.82×10^2	1.39×10^2	8.28×10^2	6.09×10^2
206	1,2-Di-(9Z,12Z,15Z-octadecatrienoyl)-3-(Galactosyl-alpha-1-6-Galactosyl-beta-1)-glycerol	9.48×10^2	1.31×10^2	6.39×10^2	2.69×10^3
207	Licoricesaponin F3	nd	nd	3.54×10^2	nd

(*continued on next page*)

Supplementary table 1. (continued)

No.	Chemical compounds	Chromatogram peak area			
		DK	HC	CH	FTJ
208	Megalomicin C1	nd	nd	nd	3.27×10^2
209	(S)-Nerolidol 3-O-[a-L-Rhamnopyranosyl-(1->4)-a-L-rhamnopyranosyl-(1->2)-[4-(4-hydroxy-3-methoxycinnamoyl)-(E)-a-L-rhamnopyranosyl-(1->6)]-b-D-glucopyranoside]	nd	1.39×10^2	nd	nd
210	PIP2(16:0/18:0)	nd	nd	nd	8.18×10^2
211	Bradykinin	nd	nd	2.26×10^3	nd
212	Undecaprenyl N-acetyl-glucosaminyl-N-acetyl-mannosaminuronate pyrophosphate	nd	nd	5.39×10^2	6.69×10^2

nd = not detected; DK = Dee pla kung, HC = Hom chang, CH = Cha hom, and FTJ = Fah talai jone.

References

[1] Somprasong W, Vjarodaya S, Chayamarit K. Taxonomic Study of the Family Acanthaceae used as traditional medicinal plants for ethnic groups in North, Central and Northeastern Thailand. Thai Agri Res J 2014;32(1):77−88.

[2] Xu Z, Chang L. Acanthaceae. In: Xu Z, Chang L, editors. Identification and control of common weeds: volume 3. Singapore: Springer Singapore; 2017. p. 329−38.

[3] Poeaim S, Lordkhem P, Charoenying P, Laipasu P. Evaluation of antioxidant, cytotoxic activities and total phenolic content from leaf extracts of Phlogacanthus pulcherrimus. Int J Agric Technol 2016;12:1657−67.

[4] Okhuarobo A, Falodun JE, Erharuyi O, Imieje V, Falodun A, Langer P. Harnessing the medicinal properties of Andrographis paniculata for diseases and beyond: a review of its phytochemistry and pharmacology. Asian Pacific J Trop Disease 2014;4(3):213−22.

[5] Aromdee C, Wichitchote P, Jantakun N. Spectrophotometric determination of total lactones in Andrographis paniculata Nees. Songklanakarin J Sci Technol 2005;27(6):1227−31.

[6] Islam MT, Ali ES, Uddin SJ, Islam MA, Shaw S, Khan IN, et al. Andrographolide, a diterpene lactone from Andrographis paniculata and its therapeutic promises in cancer. Cancer Lett 2018;420:129−45.

[7] Kumar RA, Sridevi K, Kumar NV, Nanduri S, Rajagopal S. Anticancer and immunostimulatory compounds from Andrographis paniculata. J Ethnopharmacol 2004;92(2−3):291−5.

[8] Puttarak P, Charoonratana T, Panichayupakaranant P. Antimicrobial activity and stability of rhinacanthins-rich Rhinacanthus nasutus extract. Phytomedicine 2010;17(5):323−7.

[9] Tangpong J, Satarug S. Alleviation of lead poisoning in the brain with aqueous leaf extract of the Thunbergia laurifolia (Linn.). Toxicol Lett 2010;198(1):83−8.

[10] Prathanturarug S, Soonthornchareonnon N, Chuakul W, Saralamp P. Variation in growth and diterpene lactones among field-cultivated Andrographis paniculata. J Nat Med 2007;61(2):159−63.

[11] Pholphana N, Panomvana D, Rangkadilok N, Suriyo T, Puranajoti P, Ungtrakul T, et al. Andrographis paniculata: Dissolution investigation and pharmacokinetic studies of four major active diterpenoids after multiple oral dose administration in healthy Thai volunteers. J Ethnopharmacol 2016;194:513−21.

[12] Valdiani A, Kadir MA, Tan SG, Talei D, Abdullah MP, Nikzad S. Nain-e Havandi Andrographis paniculata present yesterday, absent today: a plenary review on underutilized herb of Iran's pharmaceutical plants. Mol Biol Rep 2012;39(5):5409−24.

[13] Xie R, Lin Z, Zhong C, Li S, Chen B, Wu Y, et al. Deciphering the potential anti-COVID-19 active ingredients in Andrographis paniculata (Burm. F.) Nees by combination of network pharmacology, molecular docking, and molecular dynamics. RSC Adv 2021;11(58):36511−7.

[14] Jiang M, Sheng F, Zhang Z, Ma X, Gao T, Fu C, et al. Andrographis paniculata (Burm. f.) Nees and its major constituent andrographolide as potential antiviral agents. J Ethnopharmacol 2021;272:113954.

[15] Truong DH, Luu TN, Huynh NTA, Ngo NH, Nguyen QH, Le TT. Phlogacanthus cornutus: chemical profiles and antioxidant effects. Plant Sci Today 2023;10(1):266−71.

[16] THYRSIFLORUS P. ANTIOXIDANT ACTIVITIES OF TWO MEDICINAL VEGETABLES: PARKIA JAVANICA AND.

[17] Das BK, Al-Amin MM, Chowdhury NN, Majumder MFU, Uddin MN, Pavel MAM. Analgesic, anti-inflammatory, and anti-oxidant activities of Phlogacanthus thyrsiflorus leaves. J Basic Clin Physiol Pharmacol 2015;26(2):153−9.

[18] Seal T, Chaudhuri K. Antioxidant activities of some wild edible plants of Meghalaya state in India and effect of solvent extraction system. Int J Pharm Pharmaceut Sci 2015 01/01;7:446−50.

[19] Tiwary BK, Bihani S, Kumar A, Chakraborty R, Ghosh R. The in vitro cytotoxic activity of ethno-pharmacological important plants of Darjeeling district of West Bengal against different human cancer cell lines. BMC Compl Alternative Med 2015;15(1):1−10.

[20] Yuan X-H, Li B-G, Zhang X-Y, Qi H-Y, Zhou M, Zhang G-L. Two diterpenes and three diterpene glucosides from Phlogacanthus curviflorus. J Nat Prod 2005;68(1):86−9.

[21] Barua A, Chowdhury M, Biswas S, Gupta CD, Banerjee S, Saha S, et al. The structure and stereochemistry of phlogantholide-A, a diterpene from Phlogacanthus thyrsiflorus. Phytochemistry 1985;24(9):2037−9.

[22] Lai GF, Wang XY, Wang YF, Cao JX, Luo SD, Ju P. Diterpenes and diterpene glucosides from Phlogacanthus curviflorus. Helv Chim Acta 2009;92(3):470−80.

[23] Neuweiler R, Bertschinger L, Stamp P, Feil B. The impact of ground cover management on soil nitrogen levels, parameters of vegetative crop development, yield and fruit quality of strawberries. Eur J Hortic Sci 2003;68(4):183−91.

[24] Hoffmann WA, Poorter H. Avoiding bias in calculations of relative growth rate. Ann Bot 2002;90(1):37−42.

[25] Parekh J, Jadeja D, Chanda S. Efficacy of aqueous and methanol extracts of some medicinal plants for potential antibacterial activity. Turk J Biol 2005;29(4):203−10.

[26] Mothana RA, Lindequist U. Antimicrobial activity of some medicinal plants of the island Soqotra. J Ethnopharmacol 2005;96(1−2):177−81.

[27] Poeaim S, Lordkhem P, Charoenying P, Laipasu P. Evaluation of antioxidant, cytotoxic activities and total phenolic

content from leaf extracts of Phlogacanthus pulcherrimus. Int J Agric Technol 2016;12(1):1657−67.
[28] Bora J, Syiem D, Bhan S. Quantitative analysis of total phenolic, flavonoid contents and HPTLC fingerprinting of flower extracts of Phlogacanthus thyrsiflorus nees. J Pharmacogn Phytochem 2019;8(3):906−11.
[29] Kaur S, Mondal P. Study of total phenolic and flavonoid content, antioxidant activity and antimicrobial properties of medicinal plants. J Microbiol Exp 2014;1(1):00005.
[30] Onsa NE, Prasad SK, Chaiyaso T, Lumsangkul C, Sommano SR. Phenotypic and Chemotypic Relations among Local Andrographis paniculata (Burm. f.) Wall Landrace Collection. Horticulturae. 2022;8(10):978.
[31] Norkum ai P, Wongkaew M, Tangpao T, Sritontip P, Wongsiri S, Junmahasathien T, et al. Relationships between Phenotypes and Chemotypic Characteristics of Local Gymnema inodorum Plants in Northern Thailand. Horticulturae 2023;9(4):484.
[32] Al-Laith AA, Alkhuzai J, Freije A. Assessment of antioxidant activities of three wild medicinal plants from Bahrain. Arab J Chem 2019;12(8):2365−71.
[33] Liaqat H, Kim KJ, Park S-y, Jung SK, Park SH, Lim S, et al. Antioxidant effect of wheat germ extracts and their antilipidemic effect in palmitic acid-induced steatosis in hepg2 and 3t3-l1 cells. Foods 2021;10(5):1061.
[34] Banerjee S, Kar A, Mukherjee PK, Haldar PK, Sharma N, Katiyar CK. Immunoprotective potential of Ayurvedic herb Kalmegh (Andrographis paniculata) against respiratory viral infections−LC−MS/MS and network pharmacology analysis. Phytochem Anal 2021;32(4):629−39.
[35] Somprasong W, Vajrodaya S, Chayamarit K. Taxonomic Study of the subtribe Andrographinae, tribe Ruellieae, family Acanthaceae in Thailand. Thai Agri Res J 2015;33(1): 85−97.
[36] Phurailatpam A, Singh S, Chanu T, Ngangbam P. Phlogacanthus-An important medicinal plant of North East India: A review. Afr J Agric Res 2014;9(26):2068−72.
[37] Verma H, Negi M, Mahapatra B, Shukla A, Paul J. Evaluation of an emerging medicinal crop Kalmegh [Andrographis paniculata (Burm. F.) Wall. Ex. Nees] for commercial cultivation and pharmaceutical & industrial uses: A review. J Pharmacogn Phytochem 2019;8(4):835−48.
[38] Pearcy RW, Sims DA. Photosynthetic acclimation to changing light environments: scaling from the leaf to the whole plant. In: Exploitation of environmental heterogeneity by plants ecophysiological processes above-and belowground; 1994. p. 145−74.
[39] Poorter H, Van der Werf A, Atkin OK, Lambers H. Respiratory energy requirements of roots vary with the potential growth rate of a plant species. Physiol Plantarum 1991;83(3): 469−75.
[40] Pereyra-Irujo GA, Velázquez L, Lechner L, Aguirrezábal LA. Genetic variability for leaf growth rate and duration under water deficit in sunflower: analysis of responses at cell, organ, and plant level. J Exp Bot 2008;59(8): 2221−32.
[41] Borges CV, Minatel IO, Gomez-Gomez HA, Lima GPP. Medicinal plants: Influence of environmental factors on the content of secondary metabolites. Med Plants Environ Challeng 2017:259−77.
[42] Hassan A. Effects of mineral nutrients on physiological and biochemical processes related to secondary metabolites production in medicinal herbs. Med Aromat Plant Sci Biotechnol 2012;6(1):105−10.
[43] Van Arendonk J, Poorter H. The chemical composition and anatomical structure of leaves of grass species differing in relative growth rate. Plant Cell Environ 1994;17(8):963−70.
[44] Clements HF. Interaction of factors affecting yield. Annu Rev Plant Physiol 1964;15(1):409−42.
[45] Saeed N, Khan MR, Shabbir M. Antioxidant activity, total phenolic and total flavonoid contents of whole plant extracts Torilis leptophylla L. BMC Compl Alternative Med 2012;12: 1−12.
[46] Roy MK, Swargiary A, Verma AK. Antiproliferative and apoptosis-inducing properties of selected medicinal plants of Assam, India. Arch Med Health Sci 2021;9(2):236−43.
[47] Kripasana K, Xavier J. Phytochemical analysis and antioxidant activity of leaf extracts of some selected plants of the family Acanthaceae. Plant Sci Today 2020;7(2):264−74.
[48] Biondi F, Balducci F, Capocasa F, Visciglio M, Mei E, Vagnoni M, et al. Environmental conditions and agronomical factors influencing the levels of phytochemicals in Brassica vegetables responsible for nutritional and sensorial properties. Appl Sci 2021;11(4):1927.
[49] Poorter H, Bergkotte M. Chemical composition of 24 wild species differing in relative growth rate. Plant Cell Environ 1992;15(2):221−9.
[50] Shao J, He Y, Li F, Zhang H, Chen A, Luo S, et al. Growth inhibition and possible mechanism of oleamide against the toxin-producing cyanobacterium Microcystis aeruginosa NIES-843. Ecotoxicology 2016;25:225−33.
[51] Dimock MB, Kennedy GG, Williams WG. Toxicity studies of analogs of 2-tridecanone, a naturally occurring toxicant from a wild tomato. J Chem Ecol 1982;8:837−42.
[52] Li D, Sihamala O, Bhulaidok S, Shen L. Changes in the organic compounds following sun drying of edible black ant (Polyrhachis vicina Roger). Acta Aliment 2009;38(4):493−501.
[53] Berkey R, Bendigeri D, Xiao S. Sphingolipids and plant defense/disease: the "death" connection and beyond. Front Plant Sci 2012;3:68.
[54] Jan R, Asaf S, Numan M, Lubna Kim K-M. Plant secondary metabolite biosynthesis and transcriptional regulation in response to biotic and abiotic stress conditions. Agronomy 2021;11(5):968.
[55] Ashraf MA, Iqbal M, Rasheed R, Hussain I, Riaz M, Arif MS. Environmental stress and secondary metabolites in plants: an overview. Plant Metabol Regul Under Environ Stress 2018:153−67.
[56] Khan I, Jan S, Shinwari Z, Ali M, Khan Y, Kumar T. Ethnobotany and medicinal uses of folklore medicinal plants belonging to family Acanthaceae: An updated review. MOJ Biol Med 2017;1(2):34−8.
[57] Sudheer W, Praveen N. Phytochemical, pharmacological and tissue culture studies of some important species of the genus Barleria L.(Acanthaceae)-a review. Plant Sci Today 2021;8(3): 491−500.